Engineering Hepatocellular Morphogenesis and Function via Ligand-Presenting Hydrogels With Graded Mechanical Compliance

Eric J. Semler,[1] Perry A. Lancin,[2] Anouska Dasgupta,[1] Prabhas V. Moghe[1,2]

[1]Department of Chemical and Biochemical Engineering, Rutgers University, 98 Brett Road, Piscataway, NJ 08854; telephone: 732-445-4951; fax: 732-445-2581; e-mail: Moghe@rci.rutgers.edu
[2]Department of Biomedical Engineering, Rutgers University, 617 Bowser Road, Piscataway, NJ 08854

Abstract: In order to evaluate the sensitivity of hepatocellular cultures to variations in both substrate stiffness and bioactive ligand presentation, hepatocytes were cultured on differentially compliant polyacrylamide gel discs functionalized with varying amounts of the ECM ligand, fibronectin (FN). Subconfluent cell cultures were established in a multiwell plate format enabling the systematic evaluation of cellular response to both underlying substrate rigidity and substrate ligand concentration. Hepatocellular morphogenesis, regulated by a combination of both ligand density and substrate compliance, resulted in a broad spectrum of patterns of cellular reorganization and assembly ranging from highly two-dimensionally spread cells to highly compact, three-dimensional spheroids. Cell compaction was promoted by increasing levels of substrate mechanical compliance and generally inhibited by increasing concentrations of substrate-bound FN. We identified regimes of substrate compliance in which cells are highly responsive or relatively insensitive to the level of substrate-based ligands. For example, while FN presentation did not have a large impact on cell morphogenesis for cultures on highly compliant gels ($G' = 1.9$ kPa), hepatocytes on "firm" substrates of intermediate compliance ($G' = 5.6$ kPa) exhibited approximately a 2-fold increase in cell area between the highest and lowest FN concentrations used in this study. Further, we show that increasing substrate compliance at constant ligand concentration results in increased levels of liver-specific albumin secretion while increasing levels of FN at constant substrate rigidity yield reduced liver-specific functional activity. These substrate-elicited differences in cell function also coincided with analogous changes in the transcript levels of metabolic, growth-related, and liver-specific gene markers. Notably, these results also demonstrated that "firm" gel substrates elicit the most hepatocyte functional sensitivity to substrate-based FN presentation. Overall, our findings indicate that hepatocellular responsiveness to ligand concentration can be acutely regulated by gradation of substrate compliance, suggesting that concerted biochemical and biophysical design strategies may be critical toward the fabrication of hepatospecific biomaterials that effectively support desired levels of liver-specific function. © 2004 Wiley Periodicals, Inc.

Keywords: liver; hepatocyte; cell morphology; cell spreading; compliance; fibronectin; hydrogel

INTRODUCTION

In recent years the biophysical nature of the cellular microenvironment, in combination with its biochemical properties, has been well documented to critically modulate the outcome of three-dimensional (3D) multicellular morphogenesis during in vitro culture of anchorage-dependent cells (Alenghat and Ingber, 2002; Curtis and Riehle, 2001; Katz et al., 2000; Opas, 1989). A major challenge exists in the design of materials suitable for supporting liver-derived cell cultures, where hepatocyte morphology is known to be intimately linked to the functional output of the cells (Semler and Moghe, 2001; Singhvi et al., 1994a). Here, the maintenance of functional competence of hepatocellular cultures has often been compromised during the integration of cells with their biomaterial substrates, an event that typically induces 2D cellular structure (Bucher et al., 1990; Davis and Vacanti, 1996). To attain organ-equivalent levels of tissue function from such cultures, the design of hepatocellular constructs currently focuses not only on the underlying hepatospecific chemistry but also on the mechanosensitive nature of hepatocellular behavior in order to achieve a highly differentiated cell phenotype.

For many types of cells, specific cellular phenotypes have been previously linked to distinct patterns of cell survival, proliferation, motility, differentiation, and functional

gene expression (Huang et al., 1998; Singhvi et al., 1994b). This paradigm has been commonly observed for hepatocytes in vitro, particularly for culture systems that utilize diverse biophysical attributes to elicit markedly variant patterns of hepatocellular morphogenesis (Dispersio et al., 1991; Hamamoto et al., 1998; Hamilton et al., 2001; Hansen et al., 1994; Sawamoto and Takahashi, 1997; Singhvi et al., 1994a). Notably, hepatocyte cultures, biophysically induced to be 3D in nature, exhibit a compacted, spheroidal morphology and typically express elevated levels of liver-specific functions indicative of a highly differentiated state (Hamada et al., 1997; Hansen et al., 1998). This is in direct contrast to the levels of functional activity reported for cultures that have adopted a more 2D morphology (Baker et al., 2001; Hamamoto et al., 1998). Here, spread or elongated cells maintain a phenotypic state typically associated with increased cell growth behavior (Hansen et al., 1994).

One biophysical parameter that has been strongly implicated to determine the outcome of hepatocellular morphogenesis is the substrate mechanical compliance, as hepatocytes are believed to be highly sensitive to the mechanics of their surroundings. Previous studies have reported marked variations in hepatocyte phenotype and ensuing expression of liver-specific function upon chemical crosslinking of the underlying substrate (Coger et al., 1997; Semler et al., 2000). Here, the physical resistivity of the cellular microenvironment is believed to govern cell shape and, in turn, remodel the architecture of intracellular signaling processes (Davis et al., 2002; Geiger et al., 2001; Huang and Ingber, 2000). The effects of substrate compliance on hepatocellular behavior are also likely to be augmented by a number of biochemical factors, including soluble as well as substrate-bound hepatospecific ligands (Semler et al., 2000). To this end, we have previously utilized differentially compliant basement membrane hydrogel (Matrigel) substrates in concert with soluble growth factor stimulation in order to induce distinct patterns of hepatocellular morphogenesis and demonstrate that morphologically regulated levels of cell function can be further amplified or repressed by the presence of biochemical cues (Semler and Moghe, 2001). Despite studies such as these, few efforts have investigated the regulation of hepatocyte behavior via substrate mechanics as a function of systematic variations in substrate biochemistry.

In the current study, we developed a substrate system that can elicit diverse patterns of hepatocellular morphogenesis and function utilizing both variations in substrate mechanical compliance as well as substrate adhesivity. In order to accomplish this, as an alternative to the Matrigel system used in our previous work, we designed a differentially compliant culture system utilizing polyacrylamide-based hydrogels. These substrates possess several significant advantages, including a basal nonadhesivity to cells, the ability to have bioactive ligands covalently coupled to the gel surface (Beningo et al., 2002; Wang and Pelham, 1998), and precise control of substrate flexibility via the ratio of crosslinker monomer present upon polymerization (Pelham and Wang, 1997). For example, the differential crosslinking of polyacrylamide films can yield over 100-fold changes in their elastic storage moduli, a result that had pronounced effects on the shape and elongation of cells grown on their surfaces (Flanagan et al., 2002; Jamney et al., 2001). Recently, concerted changes in polyacrylamide gel stiffness and ligand density were also demonstrated to have profound effects on the cytoskeletal organization and cell spreading behavior of aortic smooth muscle cells (Engler et al., 2004).

For our studies, we formulated three distinct levels of mechanical compliance of polyacrylamide gel substrates, and conjugated varying levels of the highly adhesive ECM ligand, fibronectin, to the gel surface. Using a 9-condition array of these substrates, we established a wide range of hepatocellular phenotypes that had distinct levels of gene expression and liver-specific function markers. Our analysis, which focuses on understanding the cooperative effects of substrate rigidity and ligand presentation, highlights regimes of substrate stiffness in which cell morphogenesis and function are highly responsive and relatively insensitive to ligand exposure.

MATERIALS AND METHODS

Preparation of Mechanically Variant Polyacrylamide Hydrogel Discs

In order to establish a differentially compliant hepatospecific culture system, polyacrylamide hydrogels were polymerized within glass molds separated by plastic spacers (Bio-Rad, Hercules, CA), subsequently cut and adhered to the bottoms of 96-well tissue culture plates in an array-based format, and finally functionalized by covalent conjugation of fibronectin molecules. A schematic representation of this process is depicted in Figure 1. The degree of mechanical compliance of each set of hydrogels was controlled precisely by the ratio of bisacrylamide crosslinking monomers to acrylamide backbone monomers present during gel polymerization. More specifically, gels were prepared from de-aerated aqueous precursor solutions of 20% (w/v) of acrylamide monomer (Acros, Somerville, NJ) and 0.028–1.8% (w/v) of N′N′-methylene bisacrylamide monomer (Acros) using 0.5% (v/v) of N,N,N,′N′-tetramethylenediamine (TEMED) (Acros) as an accelerator and 0.5% (v/v) of 7% (w/v) ammonium persulfate (APS) (Acros) as an initiator. Immediately following APS addition and gentle swirling, 20 mL of gel precursor solutions were poured into vertical molds between two parallel glass plates (Bio-Rad) separated by 1.0-mm thick plastic spacers producing a gel of dimensions $16 \times 20 \times 0.1$ cm^3. After allowing at least 1 h for polymerization at RT to be complete, resulting gels were removed from their molds, placed in 245 square mm Bioassay Dishes (Corning, Corning, NY), and washed with excess MilliQ
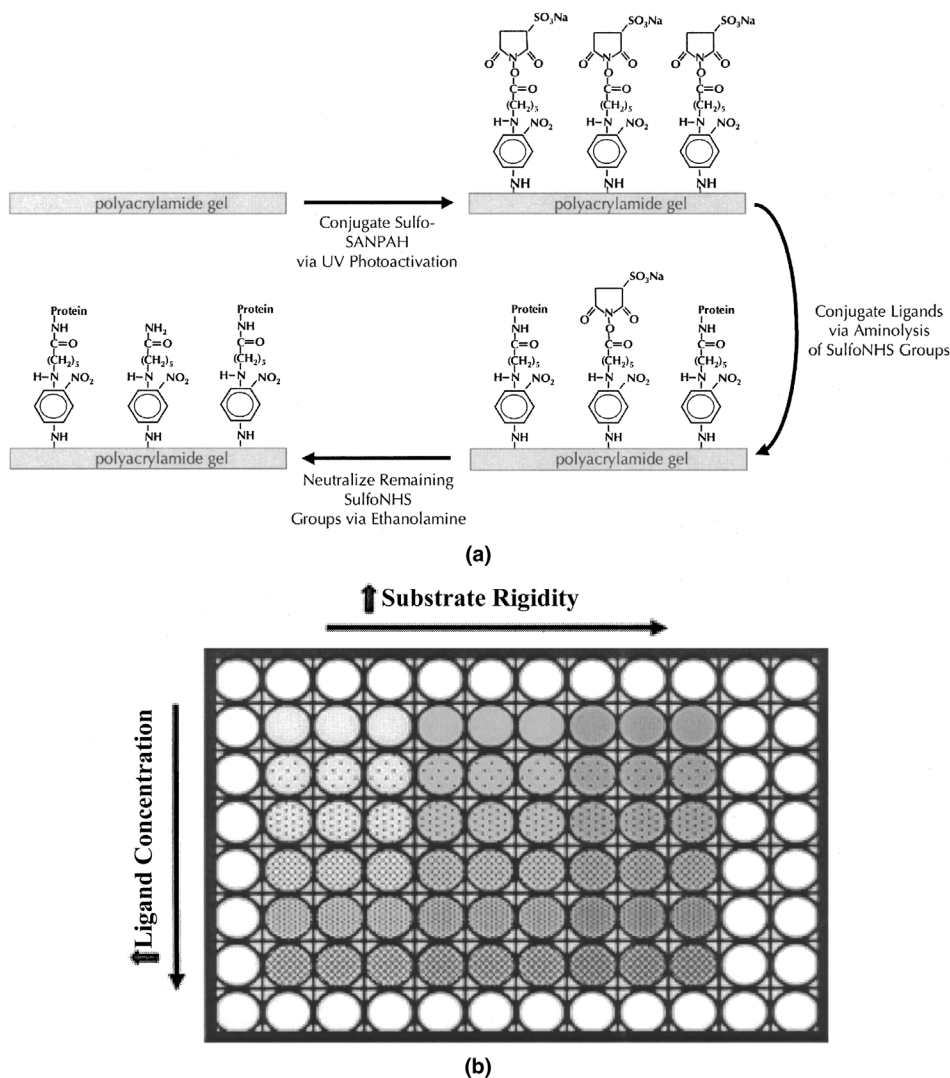
Figure 1. **a:** Schematic representation of the preparation process of ligand-presenting polyacrylamide gel disc substrates: gel surface chemistry initially following polymerization; after photoactivation with Sulfo-SANPAH; following covalent ligand binding via aminolysis of SulfoNHS; and after neutralization of any remaining active esters via ethanolamine. **b:** Diagram of array-based experimental design format for multiple assays of both ligand and substrate compliance conditions in a 96-well plate. Samples were prepared in triplicate and outer wells do not contain gels; these wells will be filled with buffer solution in order to prevent evaporation of inside wells during cell culture experiments.

H_2O several times in order to remove any unreacted monomers. Gels were then stored at least overnight in excess MilliQ H_2O in order for them to reach equilibrium swelling volumes. Subsequently, pieces of gels were removed and assayed for mechanical compliance, while the remainder of the gel slab was cut into $\frac{1}{4}''$ discs using a hole punch. This diameter (6.35 mm) is similar to that of a well inside a 96-well plate (6.4 mm). The $\frac{1}{4}''$ discs were dabbed dry and then adhered to the bottoms of 96-well plates (Nunc Nalge International, Rochester, NY) in an array-based format using a drop of optically clear glue (Norland, Cranbury, NJ). (The 36 outside wells of each 96-well plate were not utilized so that they could be filled with sterile MilliQ H_2O in order to minimize evaporation of liquid from inner wells during experiments.) In order to complete the adhesive process, plates were exposed to UV light using a Spectronics XL-1500 UV Crosslinker (Spectronics, Westbury, NY) at a distance of $2''$ for 10 min. Subsequently, affixed gel discs were washed thrice with 100 μL of MilliQ H_2O and stored in 100 μL of MilliQ H_2O until the introduction of ligands.

In order to characterize the dimensions of hydrogel discs, gel volumes were determined after equilibrium swelling had been reached via measurement of gel heights and diameters via micrometer calipers (Fisher, Pittsburgh, PA). Since more loosely crosslinked hydrogels may expand in the presence of aqueous solutions over time, hydrogel dimensions were monitored up to several days after polymerization in order to assess swelling behavior. In order to determine the water content of mechanically variant gel discs, the wet weight at equilibrium swelling conditions and the dry weight of the gel discs were compared.

Determination of Hydrogel Mechanical Compliance

The mechanical strength of polyacrylamide hydrogels was probed by obtaining rheological measurements on a SR-2000 Dynamic Stress Rheometer (Rheometrics, Piscataway, NJ), using a 25 mm cone-and-plate setup. Samples were assayed via a dynamic frequency sweep test (strain-controlled). A 23 mm cork borer (Osborne, Harrison, NJ) was utilized to punch hydrogel discs from gel slabs, and gel discs were kept in excess MilliQ H_2O at 4°C until use. To prepare samples for analysis, gel discs were placed evenly over the lower plate, which was preheated to 37°C. After allowing the gel discs several minutes to reach temperature equilibrium in this configuration, gel samples were subjected to oscillatory shear at a constant strain of 2% by rotation of the upper plate. During this frequency sweep test, viscosity and stress were measured as a function of shear rate, while during the dynamic frequency sweep both the elastic storage modulus (G′) and the loss modulus (G″) were measured as a function of angular frequency.

Activation of Polyacrylamide Gel Discs

Polyacrylamide gel discs affixed to 96-well plates were activated for subsequent ligand functionalization by adapting a protocol for preparing activated polyacrylamide sheets (Wang and Pelham, 1998). Here, ligand immobilization to polyacrylamide gel substrates was accomplished by utilizing a heterobifunctional crosslinking group, Sulfo-SANPAH (Pierce Biochemicals, Rockford, IL) that can be coupled to the gel surface following gel polymerization and then be subsequently used to covalently bind the amino groups of proteins. To prepare gel surfaces for covalent ligand coupling, hydrogel discs affixed to the bottoms of 96-well plates are overlaid with 50 μL of 0.64 mM Sulfo-SANPAH (Pierce Chemicals) in 50 mM HEPES buffer at pH 8.5 and then exposed to UV light for 5 min at a distance of 2″. After exposure to UV light, darkened Sulfo-SANPAH was removed from the gel surface and the photoactivation procedure was repeated once to ensure sufficient derivatization of the gel surface. Following this step, gels were washed four times with 100 μL of HEPES buffer for 15 min each in order to remove any unreacted Sulfo-SANPAH prior to ligand coupling. The amount of SulfoNHS groups incorporated onto hydrogel surfaces was subsequently measured via ferric hydroxamate by modifying a previously published protocol (Schnaar and Lee, 1975).

Ligand Immobilization to Activated Hydrogel Discs

Following photoactivation of gel surfaces with Sulfo-SANPAH, gels were washed and then overlaid with 100 μL of solutions of rat fibronectin (Sigma, St. Louis, MO) in 50 mM HEPES at pH 8.5 over a wide range of concentrations (bulk concentrations of 0–32 μg/mL). After allowing conjugation of ligands to hydrogel surfaces to occur overnight at 4°C under gentle agitation, gel substrates were neutralized via exposure to 100 μL of 1 M ethanolamine (Fisher) at pH 8.0 for 1 h at 4°C, converting any remaining active esters to neutral amides. Subsequently, hydrogel discs were washed thrice with a solution containing 1 M NaCl and 0.1 M KH_2PO_4 for 10 min each and then thrice with a 0.01 M KH_2PO_4 solution for 10 min each in order to remove any entrapped proteins from within the gel bulk. Finally, gel substrates were stored in 100 μL of DPBS (BioWhittaker, Walkersville, MD) at 4°C until use.

Detection of Immobilized Fibronectin

In order to detect fibronectin immobilized on hydrogel surfaces via the aminolysis of SulfoNHS groups, ELISAs were performed using a polyclonal rabbit antibody to fibronectin (Sigma). First, gel-containing wells were washed once with 100 μL of blocking buffer consisting of DPBS supplemented with 3% (v/v) normal goat serum (Sigma). Then, 100 μL of 1 μg/mL antibody solution in blocking buffer was added to each well for 1 h at RT under gentle agitation. Hydrogels were then washed 4× with 100 μL of DPBS for 10 min each. Next, 100 μL of 1:5,000 diluted HRP-conjugated goat antirabbit antibody to IgG (Sigma) in DPBS was added to each well for 1 h under gentle agitation. After this step, gel discs were again washed 4× with 100 μL of DPBS for 10 min each, and then 100 μL of OPD (o-phenylenediamine) solution prepared from a Sigmafast OPD kit (Sigma) was added above each gel for 5 min. Subsequently, 50 μL of 3 N H_2SO_4 was added to each well to quench the reaction. The optical density at 450 nm of each well was subsequently determined using a MR650 Microplate Reader (Dynatech Laboratories, Chantilly, VA), and the resulting data from each set of gel-containing wells was normalized to its corresponding background signal arising from blank gels following logarithmic transformation. A quantitative measure of fibronectin surface density was then obtained by comparing these values to standard curves generated from 96-well immunosorbent Maxisorp plates (Nunc) containing known amounts of adsorbed fibronectin. In order to properly construct standard curves, the adsorption efficiency of fibronectin on Maxisorp plates was estimated by collecting the liquid in each standard-containing well after overnight binding and transferring this volume to a fresh well that was subsequently simultaneously analyzed via ELISA. By this technique, the adsorption efficiency was determined to be ~90% for bulk fibronectin concentrations between 1–10 μg/mL, while approaching nearly 100% at concentrations less than 1 μg/mL.

Hepatocyte Isolation

Hepatocytes were isolated from adult male Fisher rats (180–220 g) under sterile conditions using a modification of a two-step perfusion procedure (Seglen, 1976). Cell yield and viability were determined via Trypan blue exclusion and hemocytometry. Typically, 250–300 million hepatocytes were harvested per rat liver with viability

ranging from 85–92%. Following isolation, cells were initially suspended in Dulbecco's minimal essential medium (DMEM) (BioWhittaker) supplemented with 10% heat-inactivated fetal bovine serum (FBS) (BioWhittaker), 20 ng/mL EGF (Sigma), 18.5 µg/mL insulin (Sigma), 7.5 µg/mL hydrocortisone (Sigma), 7 ng/mL glucagons (Sigma), 2 mM glutamine (BioWhittaker), 200 U/mL penicillin/streptomycin (BioWhittaker), and 50 µg/mL gentamycin (BioWhittaker). Cells were subsequently diluted for culture in serum-free medium. All rats were maintained and handled according to the conditions provided by the Rutgers University Institutional Review Board for the Use and Care of Animals (protocol 97-001).

Hepatocyte Culture

Prior to cell seeding, gel substrates were blocked with 100 µL of 1% (w/v) BSA (Sigma) for 2 h at 4°C and then washed thrice with 100 µL of DPBS. In order to ensure the sterility of functionalized hydrogel substrates for cell culture, 100 µL of sterile DPBS was added to each gel-containing well and plates were subsequently exposed to UV light inside a Spectronics XL-1500 UV crosslinker (Spectronics) for 30 min. Hydrogels were then washed once with 100 µL of sterile basal medium and the outer wells of the plate that did not contain gel substrates were each filled with 300 µL of sterile H_2O in order to prevent evaporation of cell culture medium from the inner wells during the course of culture. Hepatocytes were introduced to gel substrates in a volume of 100 µL of serum-free medium at a density of 3.125×10^4 cells/cm^2 (10,000 cells/well). As a positive control for hepatocyte adhesion, function, and gene expression, 1 mg/mL collagen gels were made from type I rat tail collagen (Collaborative Biomedical Products, Bedford, MA) by evenly distributing collagen at 100 µL/cm^2 in well bottoms of 96-well tissue culture plates and were used as cell substrates for extended culture. Following the first day of culture, culture medium was exchanged daily using 60 µL of serum-containing hepatocyte medium.

Characterization of Cell Morphogenesis

Cellular morphogenesis was monitored at a magnification of 10× via transmitted light microscopy using a Zeiss LSM410 laser-scanning confocal microscope (Zeiss, Thornwood, NY). At select time intervals after cell seeding, hepatocytes were viewed on gel surfaces either during culture using a stage incubator and a 5% CO_2 environment or after fixing cells with 100 µL of 3% paraformaldehyde in DPBS for 20 min at RT. After fixation, cells were washed thrice with 100 µL of DPBS and then stored in 100 µL of DPBS at 4°C prior to microscopic visualization. Several digitized images were acquired for each condition and, from each captured image, cellular spreading and elongation patterns (represented by cell area and aspect ratio, respectively) were determined for resident cells using image processing and analysis via Image Pro Plus software (Media Cybernetics, Silver Spring, MD).

Measurement of Albumin Secretion Rates

For differentially compliant polyacrylamide gel cultures, albumin secretion was measured on the third and fifth day of culture in order to assess the expression of hepatocellular differentiated function. Culture supernatants were evaluated for rat serum albumin content by using an enzyme-linked immunosorbent assay (ELISA) with purified rat albumin (ICN Pharmaceuticals, Costa Mesa, CA) and peroxidase-conjugated sheep anti-rat polyclonal antibody (ICN Pharmaceuticals). All data was obtained in triplicate and first normalized to a logarithmic curve fit of known standards and then to the numbers of viable adherent cells for each culture as determined by Calcein AM staining. Here, immediately after the culture medium was collected for a given time point, cells were washed once with 100 µL of DPBS w/Ca^{++} and Mg^{++}. Subsequently, 50 µL of 8 µM Calcein AM (Molecular Probes, Eugene, OR) was added to each well and plates were then stored at 4°C for 45 min. Following this step, plates were scanned for fluorescent intensity using a Cytofluor 4000 plate reader (Applied Biosystems, Foster City, CA) at excitation of 485 nm and emission of 520 nm. After background subtraction, data was normalized to that from collagen gel controls, where cell attachment remained at nearly 100% levels throughout the culture period.

Evaluation of Gene Expression by RT-kPCR

Three phenotypic markers (albumin, cytochrome p450, and cyclin D1) of hepatocyte cultures were evaluated on the third day of culture by implementing a kinetic reverse transcriptase chain reaction (RT-kPCR) assay using purified RNA extracts. Prior to RNA isolation, cells were washed once with 150 µL of DPBS and then total RNA was extracted from hepatocyte cultures using a High Pure RNA Isolation Kit (Roche Diagnostics, Indianapolis, IN) as per the manufacturer's instructions and kept frozen until use. The cDNA was generated by using 5 µL of extracted RNA sample and the lower primer at a concentration of 1 µM along with reagents from Access RT-PCR kits (Promega, Madison, WI) on a Powerblock I system (Ericomp, San Diego, CA). Kinetic PCR was performed on resultant cDNA using a LightCycler (Roche Diagnostics; courtesy of The Molecular Bioengineering Laboratory, Prof. Charles Roth, Rutgers University) and upper and lower primers at a concentration 0.5 µM each along with SYBR Green from a Quantitect RT-PCR Kit (Qiagen, Valencia, CA) which was utilized for fluorescent detection after each amplification cycle. For each gene target, PCR primers were annealed at 56°C and fluorescent measurements were obtained by the LightCycler for all PCR cycles at 72°C.

Based on mRNA sequences for kinetic PCR retrieved from the literature and the GenBank database, gene-specific PCR primers were designed and subsequently obtained from the DNA Synthesis and Sequencing Laboratory at UMDNJ Robert Wood Medical School (Piscataway, NJ). Including the reference gene for 18S ribosomal RNA, the gene-specific downstream primers and their annealing temperatures that were utilized in this study are given in Table I. For each experiment, all PCR amplifications were performed in duplicate and the average threshold cycle number was used to calculate fold-changes in target sample mRNA from that of control samples as follows:

$$\frac{(N_0)_{target}}{(N_0)_{control}} = (2)^{(n_{target,ref} - n_{target,gene}) - (n_{control,ref} - n_{control,gene})},$$

where N_0 is the number of initial copies and n is the threshold cycle number (Livak and Schmittgen, 2001).

Statistics

Statistical analyses were performed using unpaired t-tests assuming unequal variances and a confidence level of 95% ($P < 0.05$) was considered necessary for statistical significance. All error bars indicate the standard error around the mean.

RESULTS

Selection and Characterization of Differentially Compliant Substrates

Rheological measurements of polyacrylamide gels were performed to determine changes in mechanical properties following the variation in the amount of methylene bisacrylamide monomer in the polymer precursor solution (Fig. 2). For all gels tested, the storage modulus (G′) was invariably greater than the loss modulus (G″), and values of both moduli increased consistently with increasing crosslinking. Between the most weakly crosslinked condition (0.056% bisacrylamide crosslinker) and the most strongly crosslinked condition (3.6% bisacrylamide crosslinker) for 1-mm thick 20% acrylamide gels, over a 5-fold difference in G′ was detected using a dynamic strain-controlled
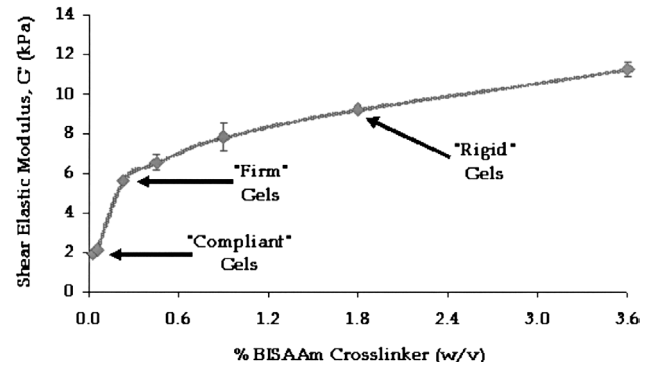

Figure 2. Mechanical properties of differentially crosslinked polyacrylamide gels containing 20% (w/v) AAm measured utilizing dynamic stress rheometry. The three gel substrate sets utilized in further studies are marked and labeled according to their macroscopic resistance to deformation.

frequency sweep at a constant 2% strain and a frequency of 1 Hz. All measurements obtained via rheometry were consistent with the macroscopic physical properties of the gels that were observed during their handling. For ensuing experiments, three crosslinking conditions were highlighted that possessed markedly different values of G′ in order to represent three distinct levels of mechanical compliance. The selected conditions contained 1.8% ("rigid" gels), 0.225% ("firm" gels), and 0.028% ("compliant" gels) of bisacrylamide crosslinker, and gel disc substrates ($^1/_4$″ diameter) prepared using these crosslinking conditions were subsequently characterized according to their equilibrium swelling properties (Table II).

Gel disc substrates were assayed to verify similar levels of ligand binding and presentation between differentially compliant samples. First, the degree of SulfoNHS conjugation to differentially compliant polyacrylamide gels following Sulfo-SANPAH photoactivation was evaluated since the incorporation of active SulfoNHS to gel surfaces is directly linked to their ability to covalently bind the protein-based ligands targeted for this study. Here, we determined that the levels of SulfoNHS conjugation (80–125 nmol/cm^2) were of the same order of magnitude for all three gel crosslinking conditions and greatly exceeded the maximal ligand densities utilized in this study (data not shown). Additionally, the ability of differentially

Table I. Primer sequences and GenBank accession numbers for targeted gene transcripts used in RT-kPCR assays.

Target	GenBank #	5′-3′ Primer sequence	Reference
18S rRNA	K01593	Upper (837) 5′-CCCGAGCCGCCTGGATAC-3′	Jayaraman et al., 2000
		Lower (1084) 5′-CCAGTCGGCATCGTTTAT-3′	
Albumin	J00698	Upper (867) 5′-TGAGAACCAGGCCACTATCTC-3′	Jayaraman et al., 2000
		Lower (1092) 5′-CTCAGCAGCAGGGACACGGAGTAA-3′	
Cyclin D1	D14014	Upper (397) 5′-TGGAGCCCCTGAAGAAGAG-3′	Kinoshita et al., 2002
		Lower (802) 5′-AAGTGCGTTGTGCGGTAGC-3′	
Cytochrome P450	L00318	Upper (46) 5′-GGTTCACACCGGCTACCAA-3′	Pan et al., 2002
		Lower (96) 5′-TGAATCTCATGGATAACTGCATCA-3′	

Table II. Characteristic properties of differentially compliant gel disc substrates.

Gel type	% BISAAm crosslinker (% w/v)	Shear modulus G' (kPa)	Equilibrium gel height (mm)	Water content (%)
"Rigid"	1.80	9.21 ± 0.08	1.09 ± 0.01	74.60 ± 0.54
"Firm"	0.225	5.63 ± 0.07	1.26 ± 0.01	89.79 ± 0.24
"Compliant"	0.028	1.93 ± 0.05	1.48 ± 0.01	93.22 ± 0.24

crosslinked Sulfo-SANPAH-derivatized polyacrylamide gel substrates to bind fibronectin (FN) via aminolysis of SulfoNHS groups was probed via ELISA techniques. The surface density of FN conjugated to activated hydrogels was shown to increase with increasing bulk FN concentration (the concentration of FN used during the gel functionalization step) and was unaffected by the level of gel crosslinking (Fig. 3). Three distinct levels of FN surface density were established from these results (0.2, 1.6, and 2.7 pmol/cm^2) and utilized in subsequent cellular studies.

Hepatocellular Morphogenesis Is Sensitive to Both Substrate Compliance and Fibronectin Density

Hepatocellular morphogenesis on differentially compliant polyacrylamide gel substrates was determined to be modulated by both gel rigidity and surface FN presentation. By 16 h of culture, cellular spreading was enhanced with increasing substrate rigidity as well as increasing FN density, although the effects of substrate mechanical compliance appeared to be more dominant (Fig. 4). In particular, in a manner independent of FN density, cells cultured on "compliant" gel substrates did not appear to undergo any significant cellular spreading (Fig. 4A–C). Hepatocytes cultured on "firm" and "rigid" gel substrates exhibited high degrees of cell spreading for FN densities of 1.6 pmol/
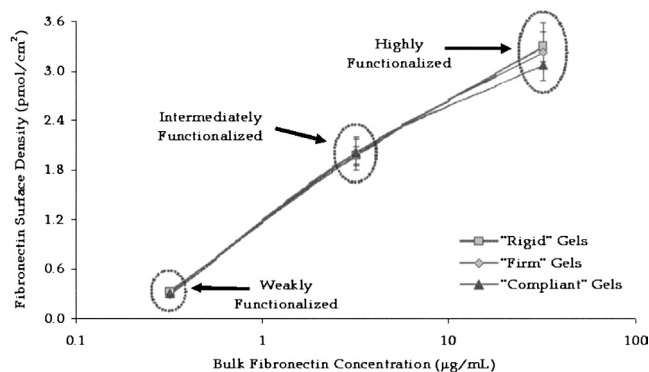

Figure 3. Detection of the levels of substrate-immobilized fibronectin via ELISA techniques for activated polyacrylamide gels of varying mechanical properties. The surface density of fibronectin coupled to gel surfaces was estimated by comparison to standard curves generated from known amounts of adsorbed fibronectin in immunosorbent 96-well plates. "Bulk" fibronectin concentration represents the fibronectin concentration utilized to coat the surface of the gel during the gel functionalization process.
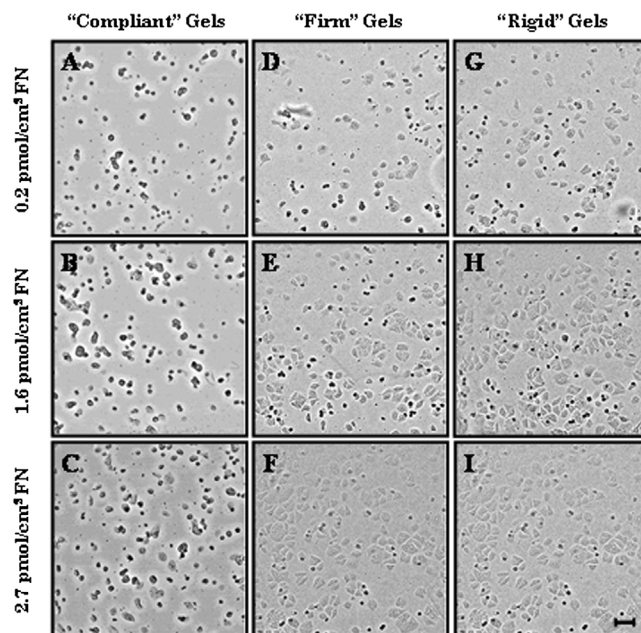

Figure 4. Transmitted light images depicting hepatocyte morphology after 16 h of culture on polyacrylamide gel substrates with varying mechanical compliance and fibronectin (FN) presentation. Gel mechanical characteristics ranged from "compliant" (**A–C**) to "firm" (**D–F**) to "rigid" (**G–I**), and the gel surface FN density varied from 0.2 (**A,D,G**) to 1.6 (**B,E,H**) to 2.7 pmol/cm^2 (**C,F,I**). Images were captured at a magnification of 10×. Scale bar = 100 μm.

cm^2 or above (Fig. 4E,F,H,I) while the degree of cellular spreading at 0.2 pmol/cm^2 FN was less pronounced on both substrates, especially on "firm" gels (Fig. 4D,G). By the third day of culture, initial cellular morphogenesis evolved into either 2D or 3D aggregation in a manner dependent on the mechanochemical characteristics of the substrate (Fig. 5). On "compliant" gel substrates (Fig. 5A–C), cells and cell aggregates remained fairly spheroidal in shape in all culture conditions, although increasing substrate-bound FN density did enhance the average size of spheroidal aggregates. On "rigid" gels (Fig. 5G–I), hepatocytes formed 2D highly interconnected aggregates for all FN conditions, although these aggregates were markedly less dense for low FN conditions. On "firm" gels, cells also formed 2D highly interconnected multicellular structures for high and intermediate FN conditions (Fig. 5E,F); however, hepatocytes at the lowest FN condition exhibited a markedly different morphology (Fig. 5D). Here, although fewer cells were clearly present, aggregates were dramatically more 3D in nature.

Hepatocellular morphogenesis was quantified for cultures on FN-functionalized, differentially compliant polyacrylamide gels by evaluating single cell area after 16 h of culture (Fig. 6). At each level of FN exposure, cellular spreading was promoted with increasing substrate rigidity. These differences were measured to be the most dramatic between cultures on "compliant" and "firm" gel substrates, where, in certain cases, nearly a 3-fold
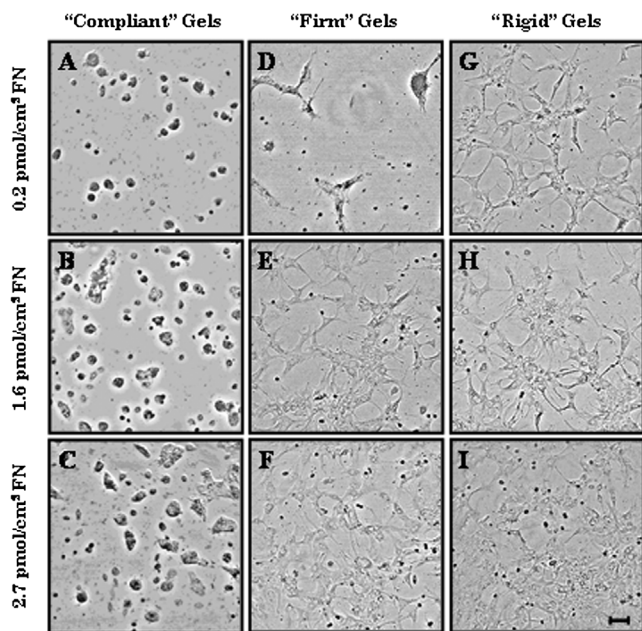
Figure 5. Transmitted light images depicting hepatocyte morphology after three days of culture on polyacrylamide gel substrates with varying mechanical compliance and fibronectin (FN) presentation. Gel mechanical characteristics ranged from "compliant" (**A–C**) to "firm" (**D–F**) to "rigid" (**G–I**), and the gel surface FN density varied from 0.2 (**A,D,G**) to 1.6 (**B,E,H**) to 2.7 pmol/cm^2 (**C,F,I**). Images were captured at a magnification of 10×. Scale bar = 100 µm.

increase was detected. In addition, increasing amounts of substrate-presented FN were determined to elicit considerable intensification of cellular spreading in a substrate rigidity-dependent manner. This phenomenon was most pronounced between cultures of intermediate fibronectin exposure (1.6 pmolcm^2) and low fibronectin exposure (0.2 pmol/cm^2) for cultures on "firm" gels engendering as much as a 47% increase in cell spreading. These effects were much less prominent for hepatocyte cultures on the other two gel substrates, particularly on "compliant" gels, where differences in cell spreading were only discernable between the higher levels of substrate-presented FN.

Albumin Secretion Is Also Modulated by Both Substrate Rigidity and Fibronectin Density

For differentially compliant polyacrylamide gel cultures, albumin secretion rates were averaged over the third and fifth days of culture in order to evaluate the expression of hepatocyte differentiated function. All data was normalized on a per-cell basis to the numbers of viable adherent cells as determined by Calcein AM staining. For hepatocellular cultures on polyacrylamide gel substrates, increasing substrate rigidity led to a reduction in albumin secretion rates independent of the amount of substrate-based FN (Fig. 7). This effect was most dramatic at levels of high (2.7 pmol/cm^2) and intermediate (1.6 pmol/cm^2) FN presentation, where a greater than 3-fold reduction in function was detected, while being significant but less pronounced at levels of low FN presentation (0.2 pmol/cm^2). Additionally, increasing levels of substrate-immobilized FN also led to a reduction in hepatocellular function. These effects were the most dramatic for cultures on "firm" gels between low FN exposure (0.2 pmol/cm^2) and intermediate FN exposure (1.6 pmol/cm^2), where a nearly 50% reduction was measured. In contrast, for hepatocyte cultures on "compliant" gel substrates the increasing presence of FN did not produce a statistically significant reduction in albumin secretion over the range of FN exposure utilized in our studies.

Mechanochemical Substrate Properties Regulate the Expression of Growth- and Metabolic/Function-Related Genes

In order to provide a quantitative measure of the cell cycle, gene expression of hepatocellular cultures was analyzed via
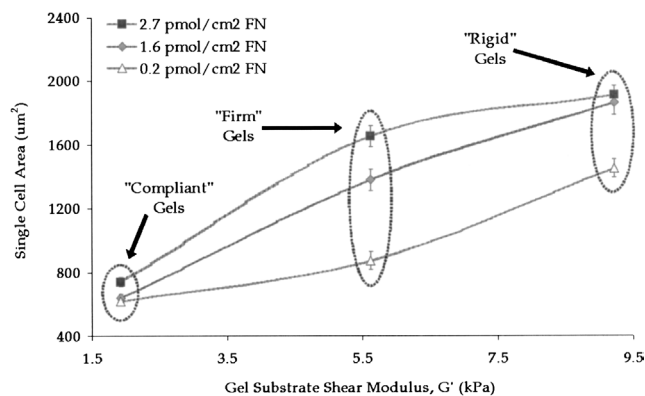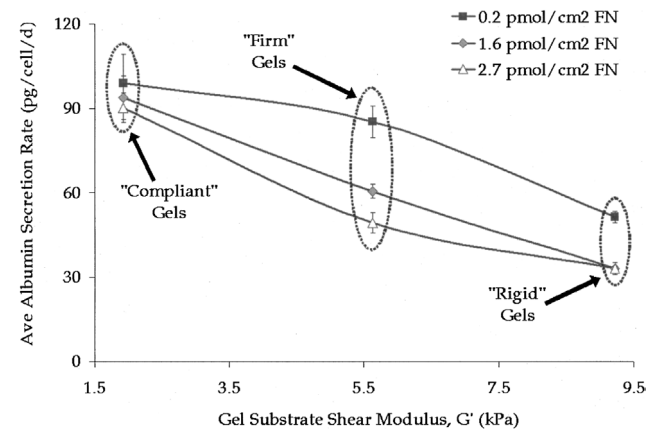

Figure 6. Effects of gel substrate rigidity on hepatocyte morphogenesis at distinct levels of exposure to substrate-immobilized fibronectin. Cell morphology was quantified in terms of single cell area that was computed after 16 h of culture for cells on "compliant," "firm," and "rigid" polyacrylamide gel substrates.

Figure 7. Effects of gel substrate rigidity on the expression of liver-specific function at distinct levels of exposure to substrate-immobilized fibronectin. Albumin secretion rates were averaged over the third and fifth days of culture for cells cultured on "compliant," "firm," and "rigid" gel substrates.

kinetic RT-PCR on the third day of cell plating. Here, genes indicative of cell growth (cyclin D1), metabolism (cytochrome p450), and liver-specific function (albumin) were analyzed, standardized using 18S rRNA as the housekeeping gene, computed as fold changes over collagen control cultures for each PCR run, and reported relative to a baseline culture condition. Here, it was determined that changes in gene expression between growth-related and metabolic/function-related genes were reciprocally related with varying substrate rigidity for all levels of FN exposure. In particular, for gel substrates functionalized with 2.7 pmol/cm² FN, albumin and p450 mRNA were detected to decrease considerably as gel substrates became more rigid, while cyclin D1 mRNA was determined to exhibit a substantial increase over the same range of substrate stiffness (Fig. 8a). Similar trends in gene expression were also detected under conditions where gel substrates were functionalized with increasing amounts of FN. Specifically, for "firm" gel substrates, which were previously determined to yield the most elastic morphogenetic and functional response to FN, increasing FN presentation was
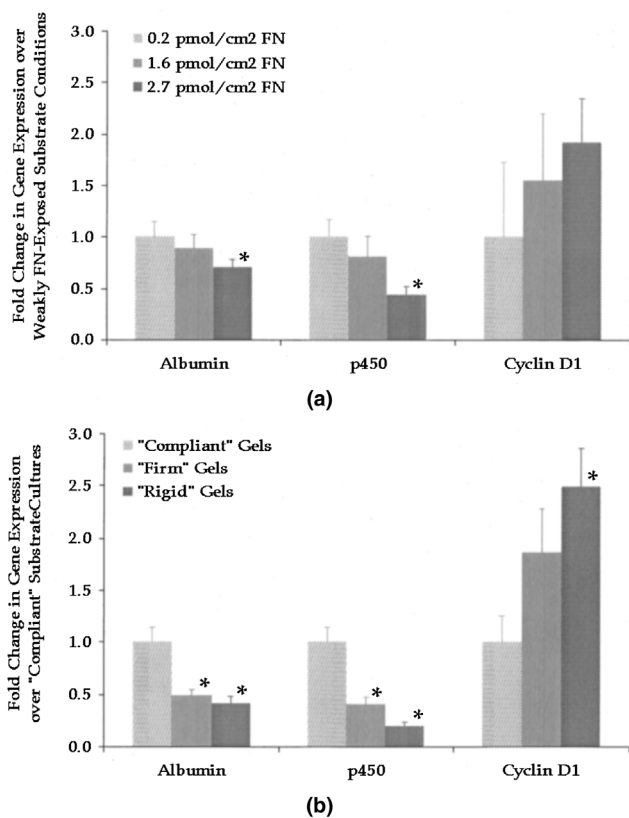

Figure 8. **a:** Effects of substrate rigidity on hepatocyte gene expression determined via quantitative RT-kPCR for cells cultured on differentially compliant gel substrates at the highest degree of substrate-displayed fibronectin (2.7 pmol/cm² FN). **b:** Effects of substrate-presented fibronectin (FN) on hepatocyte gene expression for hepatocellular cultures on "firm" polyacrylamide gel substrates. For all gene expression assays, RNA was isolated from hepatocellular cultures after 3 days of culture, 18S rRNA utilized as the housekeeping gene, and gene expression reported in fold changes relative to baseline substrate conditions in each plot.
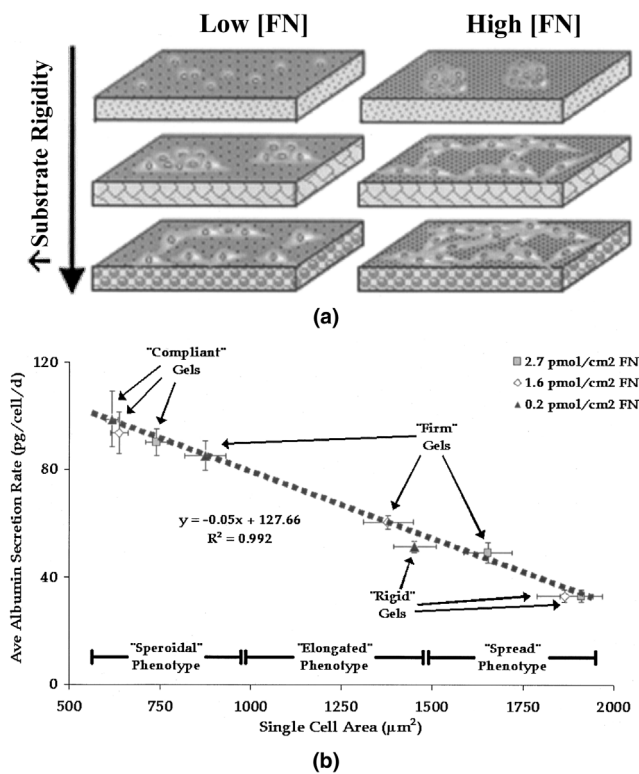
measured to promote growth-related gene expression at the expense of metabolic/function-related mRNAs (Fig. 8b). Hepatocellular cultures on "rigid" and "compliant" gels also exhibited similar, although less pronounced, patterns of gene expression upon increasing levels of substrate-immobilized FN (data not shown).

DISCUSSION

Hepatocellular morphogenesis and assembly have been well established to be critical to the functional performance of liver-derived cells in vitro (Hansen et al., 1998; Singhvi et al., 1994a; Torok et al., 2001; Yuasa et al., 1993). In this study, we offer a bidimensional approach to systematically obtain distinct cell morphogenetic and functional outcomes by manipulating both substrate mechanical compliance and substrate bioactivity (ligand concentration). To this end, we implemented a 2D array-based format of ligand-presenting, differentially compliant substrates in multiwell plates, which allows for the simultaneous evaluation of a large number of mechanochemically variant conditions. On these polyacrylamide gel-based substrates, we demonstrated an acute mechanosensitivity of hepatocyte morphogenetic and functional responses under conditions where differential levels of the adhesive ECM ligand, fibronectin, are utilized to anchor the cells to the substrate surface. These findings suggest a means to engineer diverse patterns of hepatocellular morphogenesis and subsequent expression of liver-specific function. In addition, our approach also facilitates the identification of regimes of substrate rigidity within which hepatocytes are most responsive or relatively insensitive to changes in substrate biochemistry.

Our results indicate that the systematic manipulation of substrate rigidity and ligand chemistry can yield a broad spectrum of cellular morphologies (Fig. 9a). The coordinated cellular response to both substrate compliance and substrate biochemistry was particularly apparent for hepatocytes cultured on "firm" substrates (gels of intermediate compliance), as cellular morphogenesis was the most sensitive to variations in FN density on these surfaces. These observations suggest that there may be certain regimes of substrate rigidity, such as the "firm" gels utilized in our studies, where the number of morphogenetically active cell-substrate attachment sites may be more important to the outcome of cellular morphogenesis than at other stiffness levels. In contrast, on "rigid" or "compliant" substrates, the high or low mechanical resistivity of the substrate alone can dominate the progression of cytoskeletal reorganization. This notion supports the belief that cellular morphogenesis is a result of both cytoskeleton-generated tractile forces and the resistance offered at the specific attachment sites by the surrounding matrix, which in turn is governed by the matrix stiffness and the number of adhesive ligands tethered to the matrix (Friedl et al., 1998; Tranquillo et al., 1992; Wang et al., 2002). For cells cultured on "firm" gels, the substrate is neither completely "rigid" (providing total

Figure 9. a: Cartoon schematic depicting the diverse patterns of hepatocellular morphogenesis induced by differentially compliant substrates that possess varying amounts of substrate-bound fibronectin. **b:** The points relating hepatocyte shape (in terms of single cell area) and the expression of liver-specific function (in terms of albumin secretion rates) nearly collapse onto a single trend line, as indicated by the dashed line spanning the graph.

by Cyclin D1 mRNA) was typically promoted with increasing substrate stiffness along with increasing levels of substrate-based FN at the expense of cell metabolic (p450 mRNA) and functional activity (albumin mRNA). The inverse relation between cell proliferative response and metabolic/functional activity for hepatocytes has previously been widely reported, as conditions under which cells express high levels of hepatospecific function often yield low tendencies for proliferation and vice versa (Parsons-Wingerter and Saltzman, 1993; Takehara et al., 1992). As a downstream measure of hepatocyte functional output, albumin secretion rates were also found to be modulated by both substrate rigidity and FN ligand density. In particular, the extent of albumin secretory response was significantly reduced with increasing gel stiffness independent of the level of substrate-presented FN. Additionally, increasing exposure to FN generally led to a reduction in albumin secretion especially for cultures on "firm" gels.

Interestingly, these trends in cell function were nearly identical to those observed for cell morphogenetic response on our mechanochemically variant substrates. Notably, the most pronounced cell functional response to FN exposure occurred on "firm" gel substrates where the largest variation in cell shape was coincidentally detected. Here, albumin secretion was found to be highly correlated to cell compaction (the inverse of cell spreading), as increased 2D cell spreading was typically associated with decreased functional expression. More specifically, when albumin secretion rates were plotted versus single cell area, it was determined that the points on the resultant graph nearly collapse onto a single trend line ($R^2 = 0.992$) with spheroidal cells consistently yielding the highest levels of cell function (Fig. 9b). The magnitude of the albumin secretion rates measured for these compacted phenotypes is comparable to that reported for highly differentiated 3D hepatocyte culture systems including Matrigel and collagen sandwich (Dunn et al., 1991; Moghe et al., 1997). These observations also coincide with those that we have previously obtained for differentially compliant Matrigel cultures, where cell function was maintained at near physiological levels under mechanochemical conditions that promoted cellular compaction and 3D reorganization (Semler and Moghe, 2001). Furthermore, the notion that hepatocellular phenotype may be a dominant regulatory mechanism for determining cell functional fate is consistent with reports that distinct levels of cytoskeletal tension are associated with various hepatocyte morphologies (Bhadriraju and Hansen, 2002) and that the stiffness of the cell may not only directly affect cell functional fate but also alter the underlying mechanisms through which ligand-mediated signaling can govern cell behavior (Ingber, 1997; Ingber et al., 1994). While the differential levels of cell–cell interactions induced in our current studies may also modulate cell functional fate, we did not observe any universal correlation between the extent of hepatocyte aggregation and resultant expression of liver-specific function. To potentially eliminate the effects of cell–cell contact, future

resistance to tractile forces and forcing cells to spread in order to maximize cell-substrate adhesion) nor completely "compliant" (providing little resistance to tractile forces and causing cells to remain spheroidal in shape independent of the number of cell-matrix contacts). At high FN densities on this substrate, FN, a noted hepatocyte morphogen (Bhadriraju and Hansen, 2000; Hodgkinson et al., 2000), is able to induce spreading and 2D reorganization by not only providing anchors for which cells can exert tractile forces, but also by stimulating cells for morphogenesis. However, at low FN densities on this substrate the lack of a sufficient morphogenetic signal along with marginal substrate resistivity causes cells to exhibit far less spreading behavior and forces aggregates to be more 3D in nature. Hepatocytes, under these conditions, may have a greater affinity for each other than for the weakly FN-functionalized substrate once intercellular contacts are formed.

Combinatorial variations in substrate rigidity and FN presentation also elicited distinct cell growth, metabolic, and liver-specific functional responses of hepatocytes. For example, the detection of several key target transcripts indicated that the range of mechanochemical substrate conditions utilized in this study could engender diverse patterns of gene expression. Cell growth behavior (indicated

studies aim to utilize strategic micropatterning of hepato-specific ligands in order to allow the population-level evaluation of single cells. Recently, it has been shown that micron-sized, adhesive islands possessing well-defined spatial dimensions can be established on flexible polyacrylamide gel surfaces utilizing microfabricated elastomeric membranes (Wang et al., 2002).

In order to summarize our results, we constructed a 3D surface contour plot describing cell morphogenesis and function as a function of simultaneous variations in substrate rigidity and ligand concentration (Fig. 10). This schematic highlights several key findings that we have reported including the observation that hepatocytes are most responsive to FN at intermediate levels of substrate compliance. This elasticity can be seen by examining the steepness of the curved profile across this region. Our observation that cells on the most compliant gels are relatively insensitive to FN presentation can also be noted on this plot, as cell compaction and function are maintained at high levels, independent of FN density. This result is consistent with the insensitive nature of cell response to substrate-based ECM ligands on highly compliant polyacrylamide gels recently reported for smooth muscle cells (Engler et al., 2004).

In conclusion, we have developed a 2D, array-based approach to systematically investigate the concomitant effects of substrate mechanical compliance and ligand chemistry on cell behavior. Using this system, we have demonstrated that concerted manipulation of substrate stiffness and the density of substrate-bound FN can be utilized to achieve a wide range of hepatocellular phenotypes and direct cell functional fate. In addition, we identified regimes of substrate rigidity where cells have increased morphogenetic sensitivity to FN and determined that the expression of hepatocyte differentiated function in this system appears to be predominately governed by mechanochemically induced cell morphology. Collectively, these insights suggest a strategy to control hepatocyte behavior that can be readily incorporated into the design of hepatocellular constructs for liver tissue engineering as well as for vitro organotypic systems with toxicological and regenerative applications.

References

Alenghat FJ, Ingber DE. 2002. Mechanotransduction: all signals point to cytoskeleton, matrix, and integrins. Sci STKE 2002:E6.

Baker TK, Carfagna MA, Gao H, Dow ER, Li Q, Searfoss GH, Ryan TP. 2001. Temporal gene expression analysis of monolayer cultured rat hepatocytes. Chem Res Toxicol 14:1218–1231.

Beningo KA, Lo CM, Wang YL. 2002. Flexible polyacrylamide substrata for the analysis of mechanical interactions at cell-substratum adhesions. Methods Cell Biol 69:325–339.

Bhadriraju K, Hansen LK. 2000. Hepatocyte adhesion, growth and differentiated function on RGD-containing proteins. Biomaterials 21:267–272.

Bhadriraju K, Hansen LK. 2002. Extracellular matrix- and cytoskeleton-dependent changes in cell shape and stiffness. Exp Cell Res 278:92–100.

Bucher NLR, Robinson GS, Farmer SR. 1990. Effects of extracellular matrix on hepatocyte growth and gene expression: implications for hepatic regeneration and the repair of liver injury. Semin Liver Dis 10:11–19.

Coger R, Toner M, Moghe P, Ezzell RM, Yarmush ML. 1997. Hepatocyte aggregation and reorganization of EHS matrix gel. Tissue Eng 3:375–390.

Curtis A, Riehle M. 2001. Tissue engineering: the biophysical background. Phys Med Biol 46:R47–65.

Davis MW, Vacanti JP. 1996. Toward development of an implantable tissue engineered liver. Biomaterials 17:365–372.

Davis GE, Bayless KJ, Mavila A. 2002. Molecular basis of endothelial cell morphogenesis in three-dimensional extracellular matrices. Anat Rec 268:252–275.

Dispersio CM, Jackson DA, Zaret KS. 1991. The extracellular matrix coordinately modulates liver transcription factors and hepatocyte morphology. Mol Cell Biol 11:4405–4414.

Dunn JC, Tompkins RG, Yarmush ML. 1991. Long-term in vitro function of adult hepatocytes in a collagen sandwich configuration. Biotechnol Prog 7:237–245.

Engler A, Bacakova L, Newman C, Hategan A, Griffin M, Discher D. 2004. Substrate compliance versus ligand density in cell on gel responses. Biophys J 86:617–628.

Flanagan LA, Ju YE, Marg B, Osterfield M, Janmey PA. 2002. Neurite branching on deformable substrates. Neuroreport 13:2411–2415.

Friedl P, Zanker KS, Brocker EB. 1998. Cell migration strategies in 3-D extracellular matrix: differences in morphology, cell matrix interactions, and integrin function. Microsc Res Tech 43:369–378.

Geiger B, Bershadsky A, Pankov R, Yamada KM. 2001. Transmembrane crosstalk between the extracellular matrix—cytoskeleton crosstalk. Nat Rev Mol Cell Biol 2:793–805.

Hamada T, Kato Y, Terasaki T, Sugiyama Y. 1997. Cell density-dependent mitogenic effect and -independent cellular handling of epidermal growth factor in primary cultured rat hepatocytes. J Hepatol 26:353–360.

Hamamoto R, Yamada K, Kamihira M, Iijima S. 1998. Differentiation and
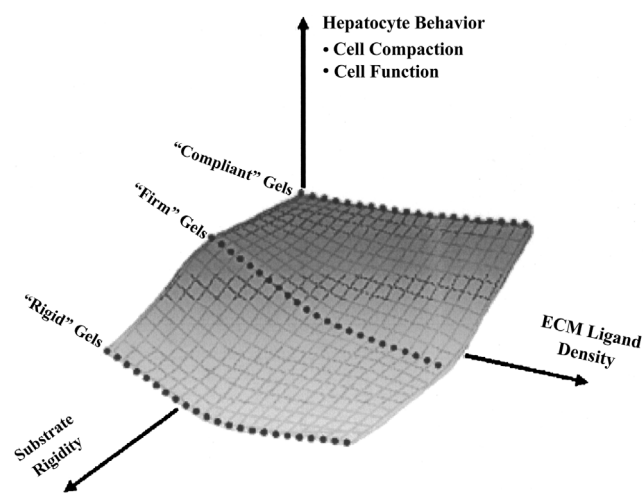
Figure 10. Cartoon schematic describing various hepatocellular phenomena as a function of substrate rigidity and density of the substrate-presented ECM ligand, fibronectin. The 3D surface contour represents both the expected spreading and functional responsiveness of hepatocytes to concerted variations in these two substrate design parameters.

proliferation of primary rat hepatocytes cultured as spheroids. J Biochem (Tokyo) 124:972–979.

Hamilton GA, Jolley SL, Gilbert D, Coon DJ, Barros S, LeCluyse EL. 2001. Regulation of cell morphology and cytochrome P450 expression in human hepatocytes by extracellular matrix and cell-cell interactions. Cell Tissue Res 306:85–99.

Hansen LK, Mooney DJ, Vacanti JP, Ingber DE. 1994. Integrin binding and cell spreading on extracellular matrix act at different points in the cell cycle to promote hepatocyte growth. Mol Biol Cell 5:967–975.

Hansen LK, Hsiao C, Friend JR, Wu FJ, Bridge GA, Remmel RP, Cerra FB, Hu W. 1998. Enhanced morphology and function in hepatocyte spheroids: A model of tissue self-assembly. Tissue Eng 4:65–74.

Hodgkinson CP, Wright MC, Paine AJ. 2000. Fibronectin-mediated hepatocyte shape change reprograms cytochrome P450 2C11 gene expression via an integrin-signaled induction of ribonuclease activity. Mol Pharmacol 58:976–981.

Huang S, Ingber DE. 2000. Shape-dependent control of cell growth, differentiation, and apoptosis: switching between attractors in cell regulatory networks. Exp Cell Res 261:91–103.

Huang S, Chen CS, Ingber DE. 1998. Control of cyclin D1, p27(Kip1), and cell cycle progression in human capillary endothelial cells by cell shape and cytoskeletal tension. Mol Biol Cell 9:3179–3193.

Ingber DE. 1997. Tensegrity: the architectural basis of cellular mechanotransduction. Annu Rev Physiol 59:575–599.

Ingber DE, Dike L, Hansen L, Karp S, Liley H, Maniotis A, McNamee H, Mooney D, Plopper G, Sims J, et al. 1994. Cellular tensegrity: exploring how mechanical changes in the cytoskeleton regulate cell growth, migration, and tissue pattern during morphogenesis. Int Rev Cytol 150:173–224.

Jamney PA, Yeung T, Flanagan LA. 2001. Effect of substrate stiffness on cell morphology. ASME Bioeng Div 50:709–710.

Jayaraman A, Yarmush ML, Roth CM. 2000. Dynamics of gene expression in rat hepatocytes under stress. Metab Eng 2:239–251.

Katz BZ, Zamir E, Bershadsky A, Kam Z, Yamada KM, Geiger B. 2000. Physical state of the extracellular matrix regulates the structure and molecular composition of cell-matrix adhesions. Mol Biol Cell 11:1047–1060.

Kinoshita A, Wanibuchi H, Imaoka S, Ogawa M, Masuda C, Morimura K, Funae Y, Fukushima S. 2002. Formation of 8-hydroxydeoxyguanosine and cell-cycle arrest in the rat liver via generation of oxidative stress by phenobarbital: association with expression profiles of p21(WAF1/Cip1), cyclin D1 and Ogg1. Carcinogenesis 23:341–349.

Livak KJ, Schmittgen TD. 2001. Analysis of relative gene expression data using real-time quantitative PCR and the 2(-Delta Delta C(T)) method. Methods 25:402–408.

Moghe PV, Coger RN, Toner M, Yarmush ML. 1997. Cell-cell interactions are essential for maintenance of hepatocyte function in collagen gel but not on matrigel. Biotechnol Bioeng 56:706–711.

Opas M. 1989. Expression of the differentiated phenotype by epithelial cells in vitro is regulated by both biochemistry and mechanics of the substratum. Dev Biol 131:281–293.

Pan J, Xiang Q, Renwick AB, Price RJ, Ball SE, Kao J, Scatina JA, Lake BG. 2002. Use of a quantitative real-time reverse transcription-polymerase chain reaction method to study the induction of CYP1A, CYP2B and CYP4A forms in precision-cut rat liver slices. Xenobiotica 32:739–747.

Parsons-Wingerter PA, Saltzman WM. 1993. Growth versus function in the three-dimensional culture of single and aggregated hepatocytes within collagen gels. Biotechnol Prog 9:600–607.

Pelham RJ Jr, Wang Y. 1997. Cell locomotion and focal adhesions are regulated by substrate flexibility. Proc Natl Acad Sci U S A 94:13661–13665.

Sawamoto K, Takahashi N. 1997. Modulation of hepatocyte function by changing the cell shape in primary culture. In Vitro Cell Dev Biol Anim 33:569–574.

Schnaar RL, Lee YC. 1975. Polyacrylamide gels copolymerized with active esters. A new medium for affinity systems. Biochemistry 14:1535–1541.

Seglen PO. 1976. Methods in cell biology. New York: Academic Press.

Semler EJ, Moghe PV. 2001. Engineering hepatocyte functional fate through growth factor dynamics: the role of cell morphologic priming. Biotechnol Bioeng 75:510–520.

Semler EJ, Ranucci CS, Moghe PV. 2000. Mechanochemical manipulation of hepatocyte aggregation can selectively induce or repress liver-specific function. Biotechnol Bioeng 69:359–369.

Singhvi R, Kumar A, Lopez GP, Stephanopoulos GN, Wang DIC, Whitesides GM, Ingber DE. 1994a. Engineering cell shape and function. Science 264:696–698.

Singhvi R, Stephanopoulos G, Wang DIC. 1994b. Review: effects of substratum morphology on cell physiology. Biotechnol Bioeng 43:764–771.

Takehara T, Matsumoto K, Nakamura T. 1992. Cell density-dependent regulation of albumin synthesis and DNA synthesis in rat hepatocytes by hepatocyte growth factor. J Biochem 112:330–334.

Torok E, Pollok JM, Ma PX, Kaufmann PM, Dandri M, Petersen J, Burda MR, Kluth D, Perner F, Rogiers X. 2001. Optimization of hepatocyte spheroid formation for hepatic tissue engineering on three-dimensional biodegradable polymer within a flow bioreactor prior to implantation. Cells Tissues Organs 169:34–41.

Tranquillo RT, Durrani MA, Moon AG. 1992. Tissue engineering science: consequences of cell traction force. Cytotechnology 10:225–250.

Wang YL, Pelham RJ Jr. 1998. Preparation of a flexible, porous polyacrylamide substrate for mechanical studies of cultured cells. Methods Enzymol 298:489–496.

Wang N, Ostuni E, Whitesides GM, Ingber DE. 2002. Micropatterning tractional forces in living cells. Cell Motil Cytoskeleton 52:97–106.

Yuasa C, Tomita Y, Shono M, Ishimura K, Ichihara A. 1993. Importance of cell aggregation for expression of liver functions and regeneration demonstrated with primary cultured hepatocytes. J Cell Physiol 156:522–530.